Available online at www.sciencedirect.com
SCIENCE DIRECT
Tetrahedron
ELSEVIER
Tetrahedron 62 (2006) 2789–2798

Structure elucidation of dicarboxylate complex of Sn^{IV} porphyrin with a ring current effect model

Hajime Iwamoto,[a] Kenji Hori[b] and Yoshimasa Fukazawa[a,*]

[a]*Department of Chemistry, Graduate School of Science, Hiroshima University, 1-3-1 Kagamiyama, Higashi-Hiroshima 739-8526, Japan*
[b]*Department of Applied Chemistry and Chemical Engineering, Faculty of Engineering, Yamaguchi University, 2-16-1 Tokiwadai, Ube 755-8611, Japan*

Received 4 October 2005; revised 24 December 2005; accepted 6 January 2006

Available online 25 January 2006

Abstract—A new simple model of porphyrin ring current effect was proposed based on a line current approximation. It can reproduce the porphyrin-induced shifts for several Sn(IV)(tpp) and Sn(IV)(oep) dicarboxylate complexes quite satisfactorily. Perpendicular arrangement of the aromatic rings in the diaromatic-carboxylate complexes of Sn(IV)(tpp) and Sn(IV)(oep) was clarified with this porphyrin ring current effect model. There are two structures, *exo* and *endo*, in solution in dinaphthalene-1- and 2- carboxylate complexes of Sn(IV)(tpp) and Sn(IV)(oep). The *exo* conformer is in dynamic equilibrium with the *endo* form in solution. Thermodynamic data of these conformational equilibria are given.

1. Introduction

Determination of significantly populated conformers in extremely flexible molecules is a matter of long-standing interest. Although the X-ray crystallographic analysis is one of the most promising methods to know the precise structure, it provides only a limited number of structures in the solid state. On the other hand, NMR spectroscopy affords much useful information for not only the structures in solution but also the dynamic equilibrium between them. Freezing the conformational equilibrium, the common method for analysis, is often not experimentally attained in highly flexible molecules. It is well known that NMR chemical shifts reflect molecular structure. Hence, variation in the local environment affects chemical shieldings, and the change in chemical shifts of nuclei caused by adjacent substituents provides valuable information about the relative arrangement of the nuclei with respect to these nearby substituents.[1] From this point of view, we have developed an efficient method for conformational analysis by using chemical shift simulation method.[2] The chemical shift changes caused by secondary induced magnetic fields due to aromatic ring current have proven effective for this purpose.[3]

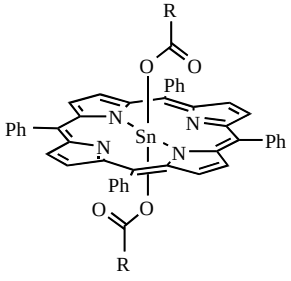

1 : R = Ph
3 : R = 1-Adamantyl
5 : R = 1-Naphthyl
7 : R = 2-Naphthyl

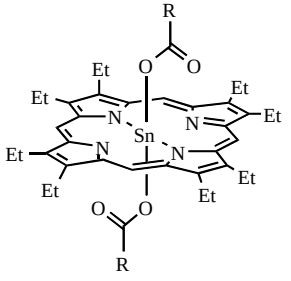

2 : R = Ph
4 : R = 1-Adamantyl
6 : R = 1-Naphthyl
8 : R = 2-Naphthyl

We have developed a new simple model of porphyrin ring current effect[4] and have succeeded for the conformational analysis of dinaphthalene-1-carboxylate complex of Sn^{IV} (tetraphenylporphyrin).[5] In this paper, we report a full account of the conformational analysis of several dicarboxylate complexes of Sn^{IV}(porphyrin), including the construction of the model of porphyrin ring current effect.

2. Results and discussion

To construct a model of porphyrin ring current effect, the established geometries of the compounds having the known induced shift values caused from porphyrin ring current effect are necessary. We utilized several dicarboxylate

Keywords: Conformation analysis; Density functional calculation; Porphyrin ring current; Structure elucidation.
* Corresponding author. Tel.: +81 82 424 7427; fax: +81 82 424 0724; e-mail: fukazawa@scic.hiroshima-u.ac.jp

0040–4020/$ - see front matter © 2006 Elsevier Ltd. All rights reserved.
doi:10.1016/j.tet.2006.01.020

complexes of Sn^{IV}(tetraphenylporphyrin), [Sn^{IV}(tpp)][6] and Sn^{IV}(octaethylporphyrin), [Sn^{IV}(oep)]. The structure of dibenzoate complex of Sn^{IV}(tpp) in the crystalline state has been reported,[7] however, that of adamantyl-1-carboxylate complex is not known. Moreover, since it is known that the structure obtained by an X-ray crystallographic analysis has lesser positional accuracy of protons than that of heavier elements, density functional theory (DFT) calculations (at the B3LYP/LANL2DZ level of theory) were carried out to have precise geometries of these compounds.[8] The structures of dicarboxylate complexes of Sn^{IV}(tpp) thus obtained have common characteristic features; (1) the orientation of the carboxylate plane (O–C═O), with respect to the porphyrin ring, (2) small tilting of Sn–O bond from the vertical axis of the porphyrin plane, (3) upward bending of one of the four peripheral phenyl rings from the porphyrin plane to have a close proximity to the carbonyl oxygen of a ligand.

2.1. Structure of dibenzoate complex of Sn^{IV}(porphyrin)

In the crystalline state, the carboxylate plane (O–C═O) of **1** is roughly perpendicular to the porphyrin ring and has eclipsed arrangement with respect to the line connecting the two diagonal *meso* carbon atoms on the porphyrin ring. The eclipsed arrangement is common in several dicarboxylate complexes of Sn^{IV}(tpp) in the crystalline state.[7,9] The benzene ring of **1** is not perpendicular to the porphyrin plane and leans ca. 25° from the normal of the plane. Similar angle of bending of the benzene ring from the porphyrin plane was observed in *m*-hydroxy benzoate complex.[7]

By contrast, the benzene ring of the calculated structure of **1** is perpendicular to the porphyrin plane (Fig. 1). The carboxylate plane, which is almost identical to that of the benzene is roughly eclipsed with respect to the line connecting the two *meso* carbons on the porphyrin ring. The Sn–O bond is not completely perpendicular to the porphyrin plane, as indicated by small deviations from right angle; N–Sn–O angles (92.4, 92.0, 87.6, 88.0°). Since the C–C bond connecting the phenyl and carboxylate groups is not parallel to the Sn–O bond, the two *ortho* aromatic protons of the benzoate are not equidistant from the porphyrin plane. One peripheral phenyl ring on the porphyrin, which is the closest to the carbonyl oxygen of the benzoate, bends upward to a detectable extent. A similar upward bending of the phenyl ring closest to the carbonyl oxygen was found in dicarboxylate complexes of Sn^{IV}(tpp) in their crystalline state.[7,9] The upward bending of the phenyl ring should be a result of an attractive interaction between the electronegative carbonyl oxygen and the *ortho* proton of the phenyl ring.[10] The diagonal phenyl ring on the porphyrin bends downward to have close proximity to the corresponding carbonyl oxygen of the *trans* benzoate. By contrast, two proximal phenyl rings bend neither upward or downward at all. Further supports of the attractive interaction can be found in the dihedral angles between the peripheral phenyl and porphyrin rings. While the two proximal phenyl rings rotate from the perpendicular position by 20°, the upward bent ring has smaller rotation angle (10°) to have a small distance from the carbonyl oxygen to the *ortho* proton of the phenyl ring.

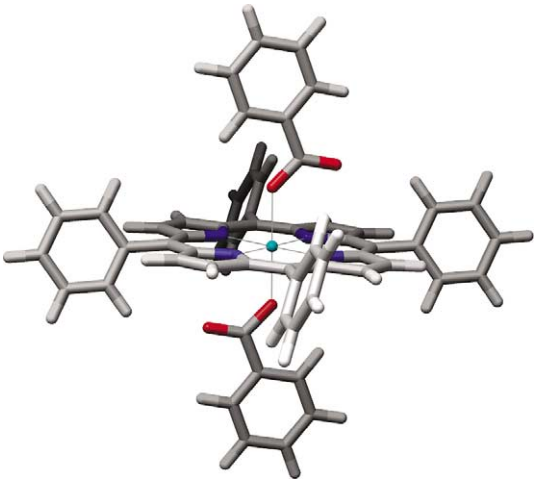

Figure 1. Molecular structure of **1** obtained from DFT calculations.

In the octaethyl porphyrin, orientation of a methyl group of each ethyl moiety can be up (*u*) or down (*d*) from the porphyrin ring. Inspection of the Cambridge crystal data base[11] suggested that an arrangement of the ethyl groups in *uuuudddd* fashion is the most frequently found one. From this reason, we employed this arrangement for the calculation of the structure of the complexes. The structural characteristics found in **1** except the upward bending of a peripheral substituent are also seen in the calculated structure of the dibenzoate complex of Sn^{IV}(oep) **2** (Fig. 2). A similar perpendicular arrangement of the benzene plane with respect to the porphyrin ring was obtained. The carboxylate plane, which is nearly identical to that of the benzene, is again roughly eclipsed with respect to the line connecting the two *meso* carbons on the porphyrin ring.

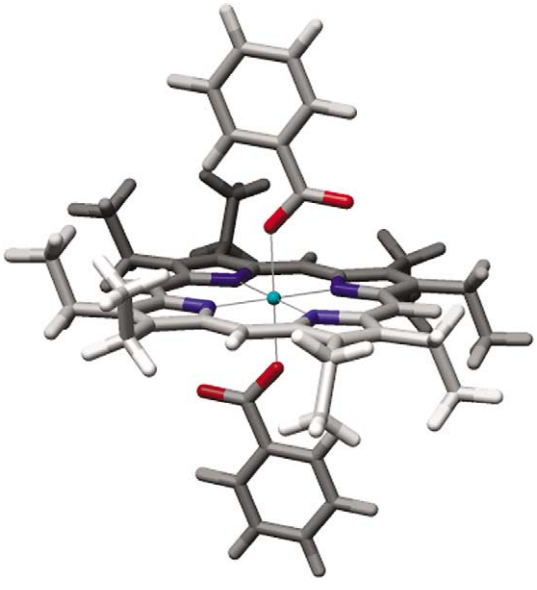

Figure 2. Molecular structure of **2** obtained from DFT calculations.

2.2. Structure of diadamantyl-1-carboxylate complex of Sn^{IV}(porphyrin)

The structural characteristics found in **1** are also found in the calculated structure of diadamantyl-1-carboxylate complex

of Sn^{IV}(tpp) **3** (Fig. 3). Small tilting of Sn–O bond from the vertical axis of the porphyrin plane was observed, as indicated by N–Sn–O angles (92.1, 91.8, 87.9, 88.2°). The carboxylate plane has roughly eclipsed arrangement with respect to the line connecting the two *meso* carbons on the porphyrin ring. The upward bending of the phenyl ring closest to the carboxylate is also observed. The dihedral angles between the peripheral phenyl and porphyrin rings indicate more clearly the attractive interaction. While the two proximal phenyl rings rotate from the perpendicular orientation by 20°, the upward bent ring has almost perpendicular arrangement; the rotation angle is only 2°.

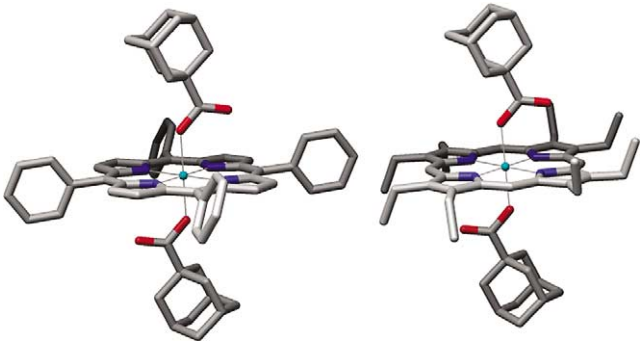

Figure 3. Molecular structures of **3** (left) and **4** (right) obtained from DFT calculations.

The tilting of Sn–O bond from the vertical axis of the porphyrin plane is conspicuous in the calculated structure of diadamantyl-1-carboxylate complex of Sn^{IV}(oep) **4**, as can be seen in N–Sn–O angles (95.3, 93.7, 85.0, 86.0°) (Fig. 3). The eclipsed arrangement of the carboxylate plane with respect to the line connecting the two *meso* carbons on the porphyrin ring was also observed in this structure.

2.3. Construction of a model of porphyrin ring current effect

Many models of porphyrin ring current effect have been reported since the first report of the NMR spectra of porphyrins by Becker and Bradley.[12] Our new model is based on a classical line current approximation as discussed originally by Salem.[13] In this simple model, the secondary magnetic field at a given proton is calculated on the assumption that the line current flows exactly through the C–C and C–N bonds of porphyrin ring. The field (H') due to the current flowing in a polygon is a sum of contributions from the edges. The magnitude of the contribution of a particular edge AB at a point P is

$$H'_{AB} = J(\sin\theta_2 - \sin\theta_1)/cR$$

where J is the line current and c is the velocity of light (Fig. 4).

In order to have induced shifts caused by the porphyrin ring current effect, estimation of the magnitude of the line current has to be given correctly. To construct the model of porphyrin ring current effect, the established geometries of the compounds having the known induced shift values caused from porphyrin ring current effect are necessary.

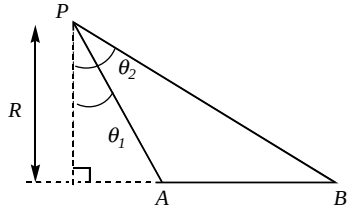

Figure 4. Calculation of magnetic field at P due to current in AB.

The chemical shift differences between the free carboxylic acid and its Sn(IV) porphyrin complex are mainly caused from two factors; complexation shift and ring current effect. It is known that the complexation shifts are negligibly small at points other than close to the site of complexation in saturated ligands.[12g] In **3** and **4**, the protons closest to the site of complexation are five bonds apart from the metal atom. Hence, the effect of the complexation shift on all the protons should be negligibly small. Similar treatment was applied to the case of the aromatic ligands, although an aromatic ligand has significant effect of the complexation shift.[12g]

Our current loop model is similar to that of Abraham's one.[12b] In this model, a current running along the two C–C bonds passing through a *meso* position separates into two (i_1, i_2) at an α-position of a pyrrole ring (Fig. 5). We employed the Abraham's ratio ($i_1/i_2=2.146$) of the two currents. We can estimate the magnitude of the line current of outer and inner arcs of the pyrrole ring ($i_1=0.87i_B$, $i_2=0.41i_B$, where i_B is the line current of benzene ring[2a]) to reproduce the ring current shift values of **1**, **2**, **3**, and **4**. Table 1 gives the observed and calculated ring current shifts in **1**, **2**, **3**, and **4**. The root mean square (rms) error is satisfactorily small (0.069 ppm). Excellent correlation of these data is obtained in a linear regression analysis [14 data (range of the observed shift, 0.81–3.53 ppm) $\Delta\delta_{obs} = a\cdot\Delta\delta_{calcd}$; $a=1.005$, $R^2=0.995$].

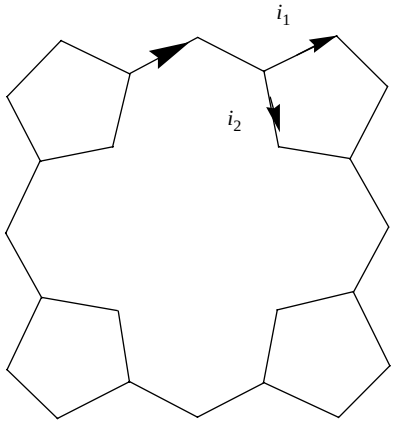

Figure 5. Current loop model for porphyrin ring.

Successful reproduction of the ring current induced shifts of the aromatic ligands in **1** and **2** with the same line current to the one, which reproduced the ring current shifts of the saturated ligands quite satisfactorily suggested clearly that our assumption of the negligible contribution of the complexation shift on the aromatic ligand is valid in these

Table 1. Observed and calculated ring-current shifts in **1**, **2**, **3**, and **4** (ppm)

Nucleus	Shifts	
	Obsd	Calcd
H_o(**1**)	3.19[a]	3.12_7
H_m(**1**)	1.15[a]	1.15_2
H_p(**1**)	0.95[a]	0.89_6
H_o(**2**)	3.53	3.42_6
H_m(**2**)	1.29	1.27_4
H_p(**2**)	1.07	0.98_4
H_2(**3**)	2.96[a]	2.90_6
H_3(**3**)	1.10[a]	1.15_6
H_{4eq}(**3**)	1.17[a]	1.22_2
H_{4ax}(**3**)	0.81[a]	0.88_6
H_2(**4**)	3.22	3.24_1
H_3(**4**)	1.22	1.28_6
H_{4eq}(**4**)	1.26	1.38_3
H_{4ax}(**4**)	0.92	0.99_8

[a] From Ref. 6.

complexes. The contour maps of the induced shift values caused from the porphyrin ring current effect are given in Figure 6 together with those of tetraphenylporphyrin. The latter is a simple sum of the shift values caused from the porphyrin ring current effect and those from the four peripheral benzene rings.

2.4. Structures of dinaphthoic-1-carboxylate complex of Sn^{IV}(tpp) 5

In order to know the structure of **5** in the crystalline state, an X-ray crystallographic analysis of **5** was carried out.[14] As can be clearly seen in Figure 7, the naphthalene ring of **5** is perpendicular to the porphyrin ring. The carboxylate plane of **5** is also perpendicular to the porphyrin ring and has roughly eclipsed arrangement with respect to the line connecting the two *meso* carbons. However, the naphthalene plane has roughly eclipsed with respect to the line connecting the two diagonal porphyrin nitrogen atoms. The small tilting of Sn–O bond from the vertical axis of the porphyrin plane was also found in this structure (N–Sn–O angles: 95.9, 92.2, 84.1, 87.8°). Also seen in this structure is the upward bending (11.2°) of one of the peripheral phenyl rings from the porphyrin plane, which is closest to the carbonyl oxygen of the ligand.

The DFT structure is slightly different from that in the crystalline state. Although, the orientations of the carboxylate planes of the two structures are quite similar with each other, those of the naphthalenes with respect to the carboxylate plane are different. The DFT structure has a smaller dihedral angle of the two planes (15.6°) than that in the crystalline state (35.7°). The common characteristic features of the Sn^{IV}(tpp) complexes are also seen in the calculated structure. The small tilting of Sn–O bond from the vertical axis of the porphyrin plane (N–Sn–O angles: 93.2, 92.2, 87.1, 87.6°) and the upward bending of one of the peripheral phenyl rings (4.4°) were found.

Since the aromatic ring of naphthalene-1-carboxylic acid is not symmetrical with respect to the arene carbonyl C–C pinched bond, two orientation of the naphthalene ring is possible. One is the orientation found in the crystal and the other is that obtained by 180° rotation around the C–C bond. The DFT calculation showed that the latter is also the energy minimum on the potential energy surface. The naphthalene ring of the latter conformer is perpendicular to the porphyrin ring. The carboxylate plane is also perpendicular and has roughly eclipsed arrangement with respect to the line connecting the two *meso* carbons. In this conformer, the dihedral angle between the naphthalene and the carboxylate planes (2.3°) is smaller than the former conformer. The small tilting of Sn–O bond from the vertical axis of the porphyrin plane was also found in this structure (N–Sn–O angles: 93.2, 93.0, 87.2, 87.6°). Small but prominent upward bending of one of the peripheral phenyl rings from the porphyrin ring (3.1°) was also found in this conformer.

2.5. Conformational analysis of 5 in solution

Two conformations, 'vertical' and 'horizontal', were proposed for the structure of aromatic carboxylate complex of Sn^{IV}(tpp).[6] In order to elucidate the structure of **5** in solution, NMR measurements of **5** at various temperatures were carried out. At room temperature two prominent signals were found at 5.29 and 4.47 ppm. These are assigned to H_2 and H_8, respectively, and are both significantly upfield shifted from the corresponding proton of the naphthalene carboxylic acid. When lower the temperature the former shifted to the lower and the latter to the higher magnetic fields (Fig. 8). This suggested that at least two conformers are in equilibrium in solution, however, it is difficult to identify how many conformers are contributing to the equilibrium because neither signal separation nor extensive signal broadening was detected down to −60 °C.

The DFT calculation disclosed that two conformers (*exo*, *endo*) are possible for **5** (Fig. 9). In order to determine the relative ratio of the two conformers in solution, the chemical shift changes caused by the porphyrin ring current was found to be very informative. Before determining the relative ratio of the two, the theoretical induced shifts of the naphthalene protons of the two DFT structures were estimated by the calculation of the porphyrin ring current effect, and they are shown in Table 2.

Excellent agreement of the calculated induced shifts with those of the observed was given when both of the conformers are present in the solution in a 64:36 (*exo*:*endo*) ratio at 25 °C. Table 3 gives the observed and calculated ring current shifts in **5**. The root mean square (rms) error is again satisfactorily small (0.076 ppm). Excellent correlation of these data is obtained in a linear regression analysis [7 data (range of the observed shift, 0.61–4.60 ppm) $\Delta\delta_{obs} = a \cdot \Delta\delta_{calcd}$; $a = 1.0124$, $R^2 = 0.997$].

The relative ratio of the two conformers is temperature dependent and the temperature variation of the relative ratio is shown in Table 4.

From this analysis, it is found that the two conformers are in dynamic equilibrium in solution; the free energy difference between the two conformers at a given temperature was obtained. Thermodynamic parameters of the equilibrium of the two conformers ($\Delta H_{endo-exo} = 1.08$ kcal/mol, $\Delta S_{endo-exo} = 2.5$ cal/mol deg) were obtained by van't Hoff plot analysis.

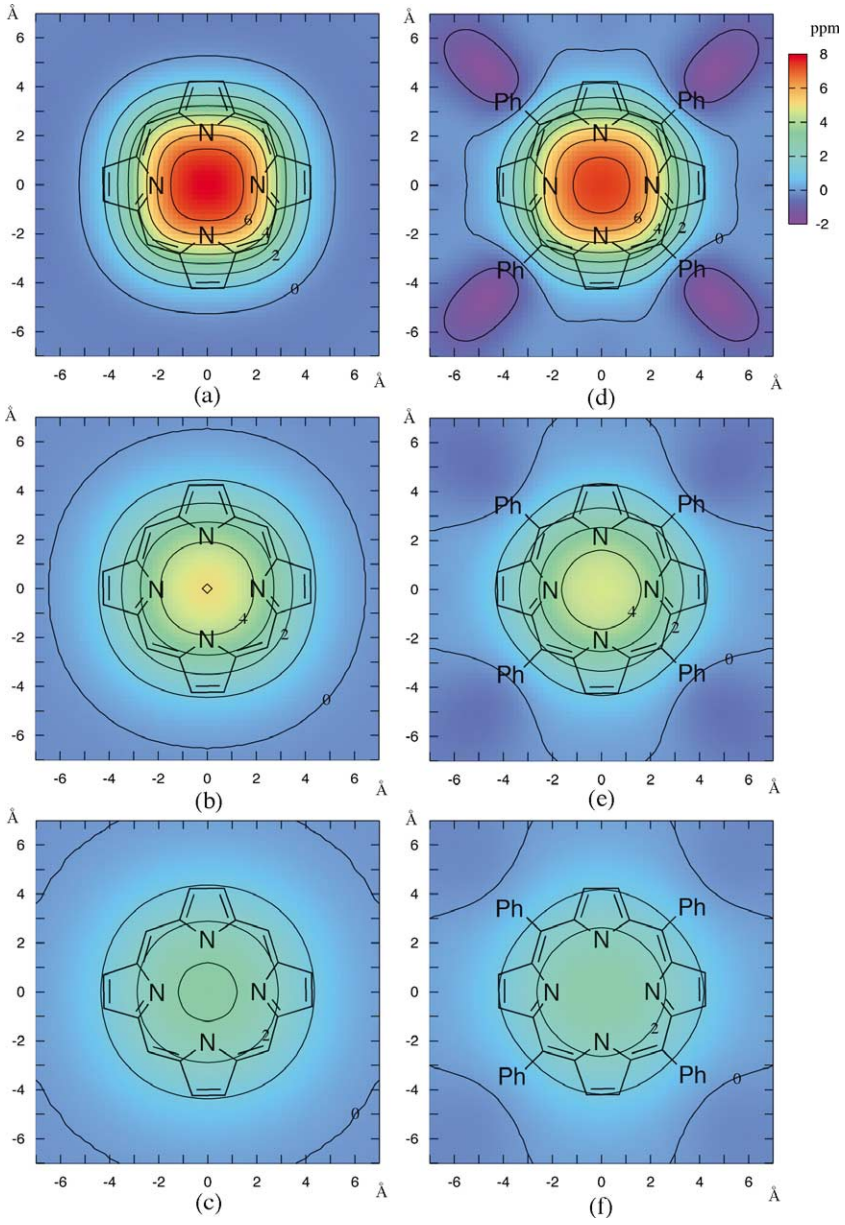

Figure 6. Contour maps of the induced shift values caused from porphyrin ring current (a) vertical section at 3.0 Å, (b) 4.0 Å, and (c) 5.0 Å. Contour maps of tetraphenylporphyrin, in which the peripheral phenyl rings have perpendicular arrangement (d) 3.0 Å, (e) 4.0 Å, and (f) 5.0 Å (ppm).

2.6. Structure and conformational analysis of dinaphthoic-1-carboxylate complexes of Sn^{IV}(oep) 6

DFT calculations of dinaphthoic-1-carboxylate complex of Sn^{IV}(oep) **6** were carried out for both the *exo* and *endo* conformations (Fig. 10). The general structural characteristics found in **5** are also seen in the calculated structures. The perpendicular arrangement of the naphthalene plane with respect to the porphyrin ring was obtained. The carboxylate plane is again perpendicular to the porphyrin and roughly eclipsed with respect to the line connecting the two *meso* carbons on the porphyrin ring. While the naphthalene plane in the *endo* structure is almost identical to the carboxylate plane that of the *exo* structure has rotated from the carboxylate plane by 14.8°. The small tilting of Sn–O bond from the vertical axis of the porphyrin plane was also found in these structures (N–Sn–O angles, *exo*: 93.1, 92.9, 86.9, 87.1°, *endo*: 92.9, 92.9, 87.1, 87.1°).

As in the case of **5**, the ^{1}H NMR spectra of **6** are temperature dependent. At room temperature two prominent signals were found at 4.42 and 4.74 ppm. These are assigned to H_2 and H_8, respectively, and are both significantly up-field shifted from the corresponding proton of the naphthalene carboxylic acid.

Excellent agreement of the calculated induced shifts with those of the observed was given when both of the conformers are present in the solution in a 48:52 (*exo*:*endo*) ratio at room temperature. The theoretical induced shifts of *exo* and *endo* conformers are given in Table 5. Table 6 gives the observed and calculated ring current shifts in **6**. The root mean square (rms) error is again satisfactorily small (0.096 ppm). Excellent correlation of these data is obtained in a linear regression analysis [7 data (range of the observed shift, 0.61–4.33 ppm) $\Delta\delta_{obs} = a \cdot \Delta\delta_{calcd}$; $a = 1.033$, $R^2 = 0.998$].

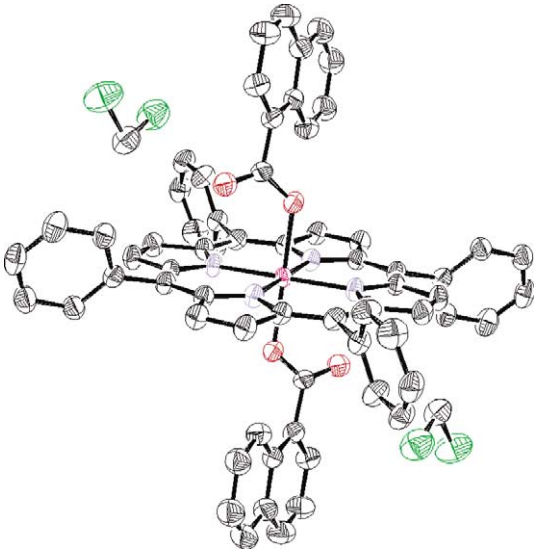

Figure 7. ORTEP drawing of **5**.

When lower the temperature H_2 peak shifted slightly and H_8 prominently to the higher magnetic field. The chemical shift differences from room temperature to −60 °C are 0.03, −0.04, −0.07, −0.06, −0.08, −0.06, and 0.23 for H_2, H_3, H_4, H_5, H_6, H_7, and H_8, respectively, (+ denotes up-field shift). The temperature dependent changes of the relative ratio of the two conformers were obtained by the chemical shift changes of these proton signals at several temperatures. Thermodynamic parameters of the equilibrium of the two conformers ($\Delta H_{endo-exo}=0.21$ kcal/mol, $\Delta S_{endo-exo}=0.9$ cal/mol deg) were obtained by van't Hoff plot analysis.

2.7. Structures and conformational analysis of dinaphthoic-2-carboxylate complexes of Sn^{IV}(tpp) 7

DFT calculation of dinaphthoic-2-carboxylate complex of Sn^{IV}(tpp) **7** was carried out for the *exo* and *endo* conformers (Fig. 11). The structural characteristics in dicarboxylate complex of Sn^{IV}(tpp) are found both in *exo* and *endo* structures. The perpendicular arrangement of the naphthoic-2-carboxylate plane to the porphyrin ring was observed with the eclipsed arrangement with respect to the line connecting the two *meso* carbons of the porphyrin ring. Upward bending of one of the peripheral benzene rings (5.5°, both of the structures) was again observed in the calculated structures. The small tilting of Sn–O bond from the vertical axis of the porphyrin plane was also found in these structures (N–Sn–O angles, *exo*: 92.4, 91.7, 87.6, 88.3°, *endo*: 92.3, 91.9, 87.7, 88.1°).

The theoretical induced shifts of the naphthalene protons of the two DFT structures were estimated by the calculation of the porphyrin ring current effect and are shown in Table 7.

Excellent agreement of the calculated induced shifts with those of the observed was given when both of the conformers are present in the solution in a 61:39 (*exo*:*endo*) ratio at 25 °C. Table 8 gives the observed and calculated ring current shifts in **7**. The root mean square (rms) error is again satisfactorily small (0.061 ppm). Excellent correlation of these data is obtained in a linear regression analysis [7 data (range of the observed shift, 0.44–3.46 ppm) $\Delta\delta_{obs}=a\cdot\Delta\delta_{calcd}$; $a=1.009$, $R^2=0.998$].

Contrary to the case of **5**, the ^{1}H NMR spectra of **7** in $CDCl_3$ did not show sizable temperature dependence down to −60 °C. The maximum shift difference (−0.05 ppm) from room temperature to −60 °C is found on H_4, H_5, and H_7; hence, the temperature variation of the ratio of the two conformers is negligibly small in this case.

2.8. Structure and conformational analysis of dinaphthoic-2-carboxylate complexes of Sn^{IV}(oep) 8

DFT calculations of dinaphthoic-2-carboxylate complex of Sn^{IV}(oep) **8** were carried out for both the *exo* and *endo* conformations (Fig. 12). In these structures, naphthalene-2-carboxylates are planar and have perpendicular arrangement to the porphyrin ring. The naphthoic-2-carboxylate planes in these conformers are eclipsed with respect to the line connecting the two *meso* carbons on the porphyrin ring.

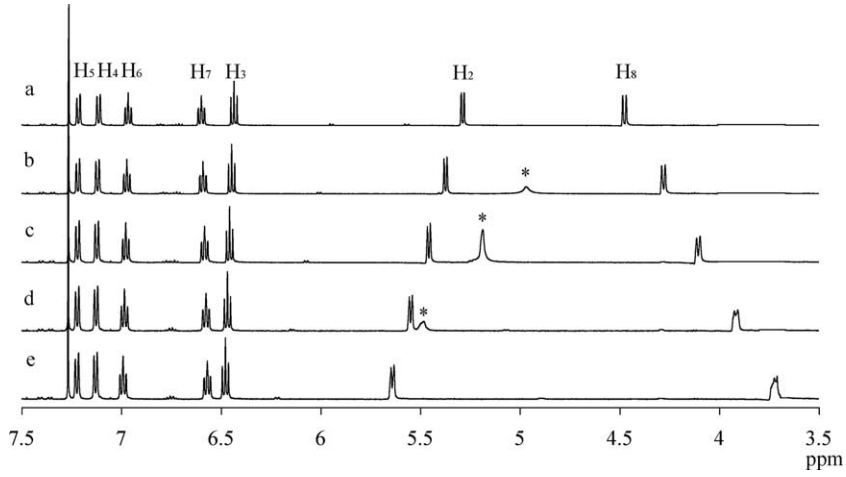

Figure 8. A part of proton NMR spectra of **5** in $CDCl_3$ at various temperatures, (a) 25 °C, (b) 0 °C, (c) −20 °C, (d) −40 °C and (e) −60 °C. * Symbols indicate signals of water.

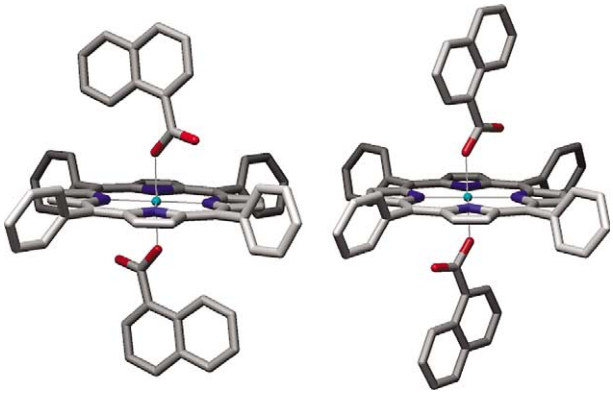

Figure 9. Molecular structures (*exo*(left), *endo*(right)) of **5** obtained from DFT calculations.

Table 2. Calculated ring-current shifts of *exo* and *endo* conformers of **5**

Nucleus	Shifts	
	exo	*endo*
H_2	2.084	4.774
H_3	0.983	1.359
H_4	0.852	0.903
H_5	0.739	0.675
H_6	0.588	0.519
H_7	1.069	0.638
H_8	6.105	1.926

Table 3. Observed (25 °C) and calculated ring-current shifts of **5** (ppm)

Nucleus	Shifts	
	Obsd	Calcd
H_2	3.10	3.05_7
H_3	1.12	1.11_9
H_4	0.98	0.87_1
H_5	0.71	0.71_6
H_6	0.61	0.56_3
H_7	1.07	0.91_3
H_8	4.60	4.59_3

Table 4. Relative ratio (%) of two conformers of **1** in $CDCl_3$

Temperature (°C)	*exo*	*endo*
25	63.8	36.2
0	67.5	32.5
−20	71.0	29.0
−40	74.5	25.5
−60	78.5	21.5

The theoretical induced shifts of the naphthalene protons of the two DFT structures were estimated by the calculation of the porphyrin ring current effect and are shown in Table 9.

Excellent agreement of the calculated induced shifts with those of the observed was given when both of the conformers are present in the solution in a 58:42 (*exo*:*endo*) ratio at 25 °C. Table 10 gives the observed and calculated ring current shifts of **8**. The root mean square (rms) error is again satisfactorily small (0.078 ppm). Excellent correlation of these data is obtained in a linear regression analysis

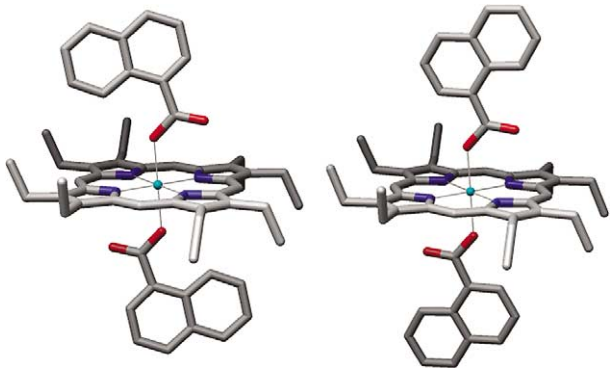

Figure 10. Molecular structures (*exo*(left), *endo*(right)) of **6** obtained from DFT calculations.

Table 5. Calculated ring-current shifts of *exo* and *endo* conformers of **6**

Nucleus	Shifts	
	exo	*endo*
H_1	2.321	5.104
H_3	1.092	1.486
H_4	0.949	0.985
H_5	0.834	0.757
H_6	0.677	0.611
H_7	1.207	0.792
H_8	6.401	2.212

Table 6. Observed (25 °C) and calculated ring-current shifts of **6** (ppm)

Nucleus	Shifts	
	Obsd	Calcd
H_2	3.97	3.77_6
H_3	1.26	1.29_8
H_4	1.02	0.96_7
H_5	0.72	0.79_4
H_6	0.61	0.64_2
H_7	1.04	0.99_0
H_8	4.33	4.21_1

[7 data (range of the observed shift, 0.49–3.76 ppm) $\Delta\delta_{obs} = a \cdot \Delta\delta_{calcd}$; $a = 1.024$, $R^2 = 0.998$].

As in the case of **7**, the ^1H NMR spectra of **8** in $CDCl_3$ does not show sizable temperature dependence down to −60 °C. The maximum shift difference from room temperature to

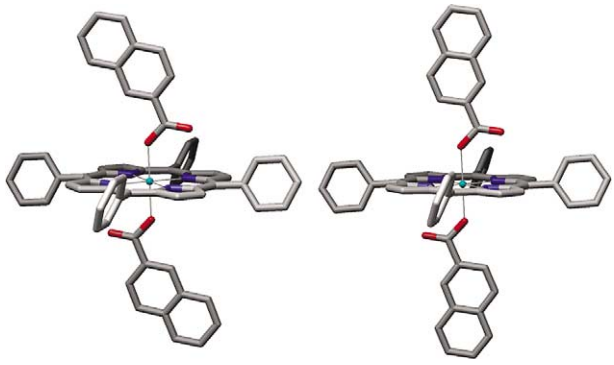

Figure 11. Molecular structures (*exo*(left), *endo*(right)) of **7** obtained from DFT calculations.

Table 7. Calculated ring-current shifts of *exo* and *endo* conformers of **7**

Nucleus	Shifts	
	exo	*endo*
H_1	4.353	1.926
H_3	2.056	4.327
H_4	1.034	1.328
H_5	0.677	0.686
H_6	0.456	0.452
H_7	0.401	0.461
H_8	1.176	0.778

Table 8. Observed (25 °C) and calculated ring-current shifts of **7** (ppm)

Nucleus	Shifts	
	Obsd	Calcd
H_1	3.46	3.39_8
H_3	3.01	2.95_0
H_4	1.11	1.15_0
H_5	0.57	0.68_1
H_6	0.44	0.45_4
H_7	0.46	0.42_5
H_8	0.96	1.01_9

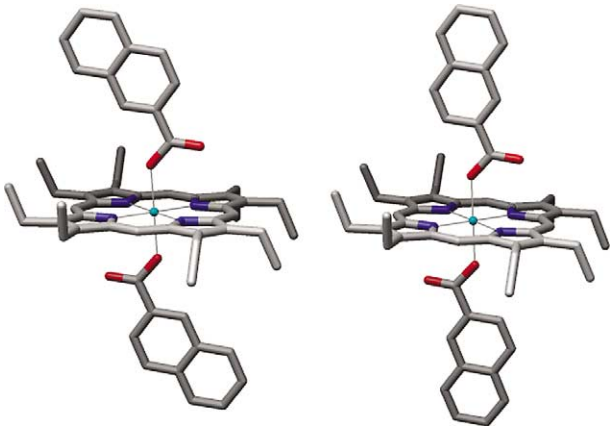

Figure 12. Molecular structures (*exo*(left), *endo*(right)) of **8** obtained from DFT calculations.

−60 °C (−0.07 ppm) is found on H_4; hence, the temperature variation of the ratio of the two conformers is negligibly small in this case.

2.9. Solvent effect

The dynamic equilibrium of the *exo* and *endo* conformers is observed in both the dinaphthoic-1- and 2-carboxylate complexes of Sn^{IV}(porphyrin). In the case of **5**, the relative ratio of the two conformers showed extensive temperature dependence in $CDCl_3$. In order to have information about the effect of the solvent on the dynamic equilibrium, the similar conformational analyses in different solvents were carried out (Table 11).

Table 9. Calculated ring-current shifts of *exo* and *endo* conformers of **8**

Nucleus	Shifts	
	exo	*endo*
H_1	4.656	2.207
H_3	2.194	4.699
H_4	1.113	1.438
H_5	0.710	0.732
H_6	0.498	0.501
H_7	0.527	0.536
H_8	1.249	0.914

Table 10. Observed (25 °C) and calculated ring-current shifts of **8** (ppm)

Nucleus	Shifts	
	Obsd	Calcd
H_1	3.76	3.63_5
H_3	3.35	3.23_8
H_4	1.25	1.24_8
H_5	0.64	0.71_9
H_6	0.50	0.49_9
H_7	0.49	0.53_1
H_8	1.03	1.10_9

Table 11. Relative ratio (%) of two conformers of **5**

Temperature (°C)	CD_2Cl_2		THF-d_8	
	exo	*endo*	*exo*	*endo*
25	58	42	57	43
0	62	38	59	41
−20	66	34	62	38
−40	69	31	65	35
−60	73	27	68	32
−90	80	20	74	26

Thermodynamic parameters of the equilibrium of the two conformers were obtained by van't Hoff plot analysis: in CD_2Cl_2, $\Delta H_{endo-exo}=0.99$ kcal/mol, $\Delta S_{endo-exo}=2.7$ cal/mol deg, in THF-d_8, $\Delta H_{endo-exo}=0.73$ kcal/mol, $\Delta S_{endo-exo}=1.9$ cal/mol deg. These thermodynamic parameters are not significantly different to those in $CDCl_3$ ($\Delta H_{endo-exo}=1.08$ kcal/mol, $\Delta S_{endo-exo}=2.5$ cal/mol deg). The enthalpy difference varies from 1.08 to 0.73 kcal/mol. The entropy differences in these solvents are all positive and do not show extensive variation regardless of the solvent, suggesting that the solvent does not play an important role in the dynamic equilibrium between *exo* and *endo* conformers in solution. The DFT vibration analysis of the two conformers in vapor phase supports this conclusion and gave a small positive entropy difference (6.2 cal/mol deg).

3. Conclusion

A new simple model of porphyrin ring current effect was given based on a classical line current approximation. It can succeed to reproduce the porphyrin-induced shifts caused from the ring current effect for several Sn^{IV}(porphyrin) dicarboxylate complexes. The successful reproduction of the porphyrin-induced shifts by using the same ring current effect for both aromatic and aliphatic ligands clarified that the complexation shift has negligible contribution to the induced shifts of the aromatic ligands. Thus, the porphyrin-induced shifts are caused from the ring current effect of the porphyrin ring. The porphyrin-induced shift values for the ligands in Sn^{IV}(tpp) dicarboxylate complexes are a simple sum of the shift values caused from the porphyrin ring current effect and those from the four perpendicular benzene rings. By contrast, those for the ligands in Sn^{IV}(oep)

dicarboxylate complexes are just from the porphyrin ring current effect, suggesting that ethyl groups on the porphyrin ring give no effect on the ring current effect.

In the DFT structure of dibenzoate complex of Sn^{IV}(porphyrin), the C–C bond connecting the phenyl and carboxylate groups is not perpendicular to the porphyrin, giving two discrete calculated induced shift values for the two *ortho* aromatic protons. Since the observed induced shift value of the *ortho* proton can be reproduced nicely with the simple average of the two calculated values, the rotation around the C–C bond connecting the phenyl and carboxylate groups is fast enough on the NMR time scale. Similar fast rotation was observed in every dicarboxylate complexes of Sn^{IV}(porphyrin). In the case of Sn^{IV}(porphyrin) complexes of asymmetric aromatic carboxylate such as 1-napathoic acid, DFT calculations gave two conformers by the rotation of the C–C bond connecting the naphtyl and carboxylate groups. The relative ratio of the two conformers was estimated by their calculated chemical induced shifts. The ratio is dependent on the temperature. The thermodynamic parameters of the conformational equilibrium were obtained by analyses of variable temperature ^{1}H NMR experiments. Thus, we have found that the ring current induced chemical shift changes of ligands are useful for the structure elucidation and conformational analysis of metalloporphyrin complexes in solution, and that the ring current induced shift values give highly reliable knowledge about the structure.

4. Experimental

4.1. General procedures

The ^{1}H and ^{13}C NMR spectra were recorded with a JEOL-ECA 600 and JEOL-Lambda 500 NMR spectrometer at 600 and 500 MHz (^{1}H NMR) and 150 and 125.65 MHz (^{13}C NMR). All NMR experiments were obtained using the standard pulse programs and sequences. The mass spectra were taken with a Simadzu MALDI-TOFMS AXIMA-CFR plus at the Instrument center for Chemical Analysis, Hiroshima University.

4.1.1. Dihydroxo(5,10,15,20-tetraphenylporphyrinato)-tin(IV). This compound was prepared by using the reported proccedure.[15]

4.1.2. Dihydroxo(2,3,7,8,12,13,17,18-octaethylporphyrinato)-tin(IV). 2,3,7,8,12,13,17,18-Octaethylporphyrin (64.7 mg, 0.12 mmol) was dissolved in pyridine (10 ml) and tin(II) chloride dihydorate (254.4 mg, 1.22 mmol) was added and the mixture heated to reflux for 9 h. Excess water was added to precipitate the product which was the filtered, washed with water. Potassium carbonate (200 mg, 1.45 mmol) and the product were dissolved in a mixture of tetrahydrofuran (40 ml) and water (10 ml) and heated to reflux for 6 h. The organic solvent was removed and the aqueous layer was extracted with dichloromethane. The organic layer was washed with water and then dried over anhydrous sodium sulfate, filtered and then the solvent was removed to give the crude product, which was recrystallized (hexane/dichloromethane 1:1) to give dihydroxo(2,3,7,8,12,13,17,18-octaethylporphyrinato)-tin(IV) (40.2 mg, 0.059 mmol, 48%) as metallic purple crystalline solids that were suitable for X-ray analysis (CCDC 274126). ^{1}H NMR (600 MHz, $CDCl_3$) δ 10.48 (s, 4H), 4.20 (q, J= 7.8 Hz, 8H), 2.03 (t, J=7.8 Hz, t). ^{13}C NMR (125.65 MHz, $CDCl_3$) δ 143.9, 143.3, 97.3, 19.9, 18.5. MALDI-TOF m/z 669.265 [$(M-OH)^+$ requires 669.262].

4.2. General method of NMR experiment

Tin porphyrin (0.003 mmol) was added to a solution of carboxylic acid (0.01 mmol) in $CDCl_3$ (1.0 ml). The mixture was sonicated at room temperature for 1 h. After 24 h, chemical shifts of dicarboxylate complex of Sn^{IV}porphyrin were measured.

Acknowledgements

We are grateful to Prof. Katsuhiko Miyoshi of Hiroshima University for his helpful discussion. This work was carried out with the support of the Grant-in Aid for Scientific Research (No. 15350025) from the Ministry of Education, Science, Sports, and Culture, Japan, which is gratefully acknowledged.

Supplementary data

Supplementary data associated with this article can be found, in the online version, at doi:10.1016/j.tet.2006.01.020.

References and notes

1. (a) ApSimon, J. W.; Craig, W. G.; Demarco, P. V.; Mathieson, D. W.; Saunders, L.; Whalley, W. B. *Tetrahedron* **1967**, *23*, 2339–2355. (b) ApSimon, J. W.; Craig, W. G.; Demarco, P. V.; Mathieson, D. W.; Saunders, L.; Whalley, W. B. *Tetrahedron* **1967**, *23*, 2357–2373. (c) ApSimon, J. W.; Craig, W. G.; Demarco, P. V.; Mathieson, D. W.; Whalley, W. B. *Tetrahedron* **1967**, *23*, 2375–2388. (d) ApSimon, J. W.; Demarco, P. V.; Mathieson, D. W.; Craig, W. G.; Karim, A.; Saunders, L.; Whalley, W. B. *Tetrahedron* **1970**, *26*, 119–146. (e) ApSimon, J. W.; Beierbeck, H. *Can. J. Chem.* **1971**, *49*, 1328–1334. (f) ApSimon, J. W.; Beierbeck, H.; Todd, D. K. *Can. J. Chem.* **1972**, *50*, 2351–2356. (g) Asakura, T.; Niizawa, Y.; Williamson, M. P. *J. Magn. Reson.* **1992**, *98*, 646–653. (h) Osapay, K.; Case, D. A. *J. Am. Chem. Soc.* **1991**, *113*, 9436–9444. (i) Sitkoff, D.; Case, D. A. *J. Am. Chem. Soc.* **1997**, *119*, 12262–12273. (j) Yang, Y.; Haino, T.; Usui, S.; Fukazawa, Y. *Tetrahedron* **1996**, *52*, 2325–2336. (k) Fukazawa, Y.; Yang, Y.; Hayashibara, T.; Usui, S. *Tetrahedron* **1996**, *52*, 2847–2862. (l) Fukazawa, Y.; Haino, T.; Kondoh, Y. *Tetrahedron Lett.* **1999**, *40*, 3591–3594. (m) Iwamoto, H.; Kawatani, T.; Fukazawa, Y. *Tetrahedron Lett.* **2001**, *42*, 1551–1553. (n) Iwamoto, H.; Kondo, Y.; Kawatani, T.; Haino, T.; Fukazawa, Y. *Tetrahedron Lett.*

2003, *44*, 5975–5978. (o) Iwamoto, H.; Kawatani, T.; Fukazawa, Y. *Tetrahedron* **2005**, *61*, 3691–3696.

2. (a) Fukazawa, Y.; Ogata, K.; Usui, S. *J. Am. Chem. Soc.* **1988**, *110*, 8692–8693. (b) Okajima, T.; Wang, Z. H.; Fukazawa, Y. *Tetrahedron Lett.* **1989**, *30*, 1551–1554. (c) Okajima, T.; Wang, Z. H.; Fukazawa, Y. *Chem. Lett.* **1991**, 37–40. (d) Fukazawa, Y.; Deyama, K.; Usui, S. *Tetrahedron Lett.* **1992**, *33*, 5803–5806. (e) Wang, Z. H.; Usui, S.; Fukazawa, Y. *Bull. Chem. Soc. Jpn.* **1993**, *66*, 1239–1243. (f) Fukazawa, Y.; Usui, S.; Tanimoto, K.; Hirai, Y. *J. Am. Chem. Soc.* **1994**, *116*, 8169–8175. (g) Iwamoto, H.; Yang, Y.; Usui, S.; Fukazawa, Y. *Tetrahedron Lett.* **2001**, *42*, 49–51.
3. (a) Waugh, J. S.; Fessenden, R. W. *J. Am. Chem. Soc.* **1957**, *79*, 846–849. (b) Johnson, C. E. J.; Bovey, F. A. *J. Chem. Phys.* **1958**, *29*, 1012–1014. (c) Perkins, S. J. *J. Magn. Reson.* **1980**, *38*, 297–312. (d) Abraham, R. J.; Leighton, P.; Sanders, J. K. M. *J. Am. Chem. Soc.* **1985**, *107*, 3472–3478. (e) Leighton, P.; Cowan, J. A.; Abraham, R. J.; Sanders, J. K. M. *J. Org. Chem.* **1988**, *53*, 733–740. (f) Sanders, G. M.; Van Dijk, M.; Van Veldhuizen, A.; Van der Plas, H. C.; Hofstra, U.; Schaafsma, T. J. *J. Org. Chem.* **1988**, *53*, 5272–5281. (g) Gust, D.; Moore, T. A.; Liddell, P. A.; Nemeth, G. A.; Makings, L. R.; Moore, A. L.; Barrett, D.; Pessiki, P. J.; Bensasson, R. V.; Rougée, M.; Chachaty, C.; De Schryver, F. C.; Van der Auweraer, M.; Holzwarth, A. R.; Connolly, J. S. *J. Am. Chem. Soc.* **1987**, *109*, 846–856. (h) Iwamoto, H.; Kawatani, T.; Fukazawa, Y. *Tetrahedron Lett.* **2001**, *42*, 1551–1553.
4. Iwamoto, H.; Hori, K.; Fukazawa, Y. *Tetrahedron Lett.* **2005**, *46*, 731–734.
5. Iwamoto, H.; Fukazawa, Y. *Heterocycles* **2005**, *65*, 523–529.
6. Hawley, J. C.; Bampos, N.; Sanders, J. K. M.; Abraham, R. J. *Chem. Commun.* **1998**, 661–662.
7. Smith, G.; Arnold, D. P.; Kennard, C. H. L.; Mak, T. C. W. *Polyhedron* **1991**, *10*, 509–516.
8. Frisch M. J. ; Trucks, G. W.; Schlegel, H. B.; Scuseria, G. E.; Robb, M. A.; Cheeseman, J. R.; Zakrzewski, V. G.; Montgomery, J. A., Jr.; Stratmann, R. E.; Burant, J. C.; Dapprich, S.; Millam, J. M.; Daniels, A. D.; Kudin, K. N.; Strain, M. C.; Farkas, O.; Tomasi, J.; Barone, V.; Cossi, M.; Cammi, R.; Mennucci, B.; Pomelli, C.; Adamo, C.; Clifford, S.; Ochterski, J.; Petersson, G. A.; Ayala, P. Y.; Cui, Q.; Morokuma, K.; Malick, D. K.; Rabuck, A. D.; Raghavachari, K.; Foresman, J. B.; Cioslowski, J.; Ortiz, J. V.; Baboul, A. G.; Stefanov, B. B.; Liu, G.; Liashenko, A.; Piskorz, P.; Komaromi, I. Gomperts, R.; Martin, R. L.; Fox, D. J.; Keith, T.; Al-Laham, M. A.; Peng, C. Y.; Nanayakkara, A.; Gonzalez, C.; Challacombe, M.; Gill, P. M. W.; Johnson, B. G.; Chen, W.; Wong, M. W.; Andres, J. L.; Head-Gordon, M.; Replogle, E. S.; Pople, J. A. *Gaussian 98;* Gaussian, Inc.: Pittsburgh PA, 1998.
9. (a) Belcher, W. J.; Brothers, P. J.; Rickard, C. E. F. *Acta Crystallogr., Sect. C* **1997**, *53*, 725–726. (b) Liu, I. C.; Lin, C.; Chen, J.; Wang, S. *Polyhedron* **1996**, *15*, 459–463.
10. (a) Taylor, R.; Kennard, O. *J. Am. Chem. Soc.* **1982**, *104*, 5063–5070. (b) Sarma, J. A. R. P.; Desiraju, G. R. *J. Chem. Soc., Perkin Trans. 2* **1987**, 1195–1202. (c) Suzuki, T.; Fujii, H.; Miyashi, T.; Yamashita, Y. *J. Org. Chem.* **1992**, *57*, 6744–6748.
11. The Cambridge Structural Database: a quarter of a million crystal structures and rising, Allen, F. H. *Acta Crystallogr., Sect. B* **2002**, *58*, 380–388.
12. (a) Becker, E. D.; Bradley, R. B. *J. Chem. Phys.* **1959**, *31*, 1413–1414. (b) Abraham, R. J. *Mol. Phys.* **1961**, *4*, 145–152. (c) Abraham, R. J.; Fell, S. C. M.; Smith, K. M. *Org. Magn. Reson.* **1977**, *9*, 367–373. (d) Abraham, R. J.; Fell, S. C. M.; Pearson, H.; Smith, K. M. *Tetrahedron* **1979**, *35*, 1759–1766. (e) Abraham, R. J.; Bedford, G. R.; McNeillie, D.; Wright, B. *Org. Magn. Reson.* **1980**, *14*, 418–425. (f) Abraham, R. J.; Smith, K. M. *J. Am. Chem. Soc.* **1983**, *105*, 5734–5741. (g) Abraham, R. J.; Medforth, C. J. *Magn. Reson. Chem.* **1987**, *25*, 432–438. (h) Abraham, R. J.; Medforth, C. J. *Magn. Reson. Chem.* **1987**, *25*, 790–797. (i) Abraham, R. J.; Medforth, C. J. *Magn. Reson. Chem.* **1988**, *26*, 803–812. (j) Abraham, R. J.; Medforth, C. J.; Mansfield, K. E.; Simpson, D. J.; Smith, K. M. *J. Chem. Soc., Perkin Trans. 2* **1988**, 1365–1370. (k) Abraham, R. J.; Rowan, A. E.; Goff, D. A.; Mansfield, K. E.; Smith, K. M. *J. Chem. Soc., Perkin Trans. 2* **1989**, 1633–1641. (l) Abraham, R. J.; Medforth, C. J. *Magn. Reson. Chem.* **1990**, *28*, 343–347. (m) Abraham, R. J.; Marsden, I. *Tetrahedron* **1992**, *48*, 7489–7504. (n) Medforth, C. J.; Muzzi, C. M.; Shea, K. M.; Smith, K. M.; Abraham, R. J.; Jia, S.; Shelnutt, J. A. *J. Chem. Soc., Perkin Trans. 2* **1997**, 839–844. (o) Gomila, R. M.; Quinonero, D.; Rotger, C.; Garau, C.; Frontera, A.; Ballester, P.; Costa, A.; Deya, P. M. *Org. Lett.* **2002**, *4*, 399–401.
13. Longuet-Higgins, H. C.; Salem, L. *Proc. Roy. Soc. (London)* **1960**, *A257*, 445–456.
14. The crystal data for $\mathbf{5}\cdot 2CH_2Cl_2$ are as follows; $\mathbf{5}\cdot 2CH_2Cl_2$: $C_{66}H_{42}N_4O_4Sn\cdot 2CH_2Cl_2$, $F_W=1240.62$, triclinic, space group $P-1$ with $a=8.6600(5)$ Å, $b=12.1150(8)$ Å, $c=15.0710(7)$ Å, $\alpha=104.541(4)$, $\beta=104.088(4)$, $\gamma=104.171(2)°$, $V=1403.48(14)$ Å^3, and $Z=1$. Data were collected at 298 K on a Mac Science DIP2030 imaging plate equipped with graphite-monochromated Mo Kα radiation ($\lambda=0.71073$ Å). Unit cell parameters were determined by auto-indexing several images in each data set separately with the program DENZO. For each data set, rotation images were collected in 3° increments with a total rotation of 180° about ϕ. Data were processed by using SCALEPACK. (The programs DENZO and SCALEPACK are available from Mac Science Co., Z. Otwinowski, University of Texas, Southwestern Medical Center.) Of 5813 total unique reflections, 5010 were considered observed at the level of $|Fo|>4.0\sigma|Fo|$. On WinGX (Farrugia, L. J., *J. Appl. Crystallogr.* **1999**, *32*, pp 837–838), the structures were solved by the direct method (SIR-97, Altomare, A.; Burla, M. C.; Camalli, M.; Cascarano, G. L.; Giacovazzo, C.; Guagliardi, A.; Moliterni, A. G. G. Polidori, G.; Spagna, R., *J. Appl. Crystallogr.* **1999**, *32*, pp 115–119) and refined by full-matrix least squares refinements on F^2 (Sheldrick, G. M. *SHELXL-97*: Program for the Refinement of Crystal Structures, University of Göttingen: Göttingen, Germany, 1997). All non-hydrogen atoms were refined anisotropically, and all hydrogen atoms were placed using AFIX instructions. The structure converged with $R=0.1029$, $wR=0.2311$. Crystallographic results have been deposited with the Cambridge Crystallographic Data Centre, UK as supplementary publication number CCDC No. 256448. Copy of the data can be obtained, free of charge, on application to CCDC, 12 Union Road, Cambridge CB2 1EZ, UK; fax: +44 1223 336033 or e-mail: data_request@ccdc.cam.ac.uk.
15. Crossley, M. J.; Thordarson, P.; Wu, R. A. S. *J. Chem. Soc., Perkin Trans. 1* **2001**, 2294–2302.